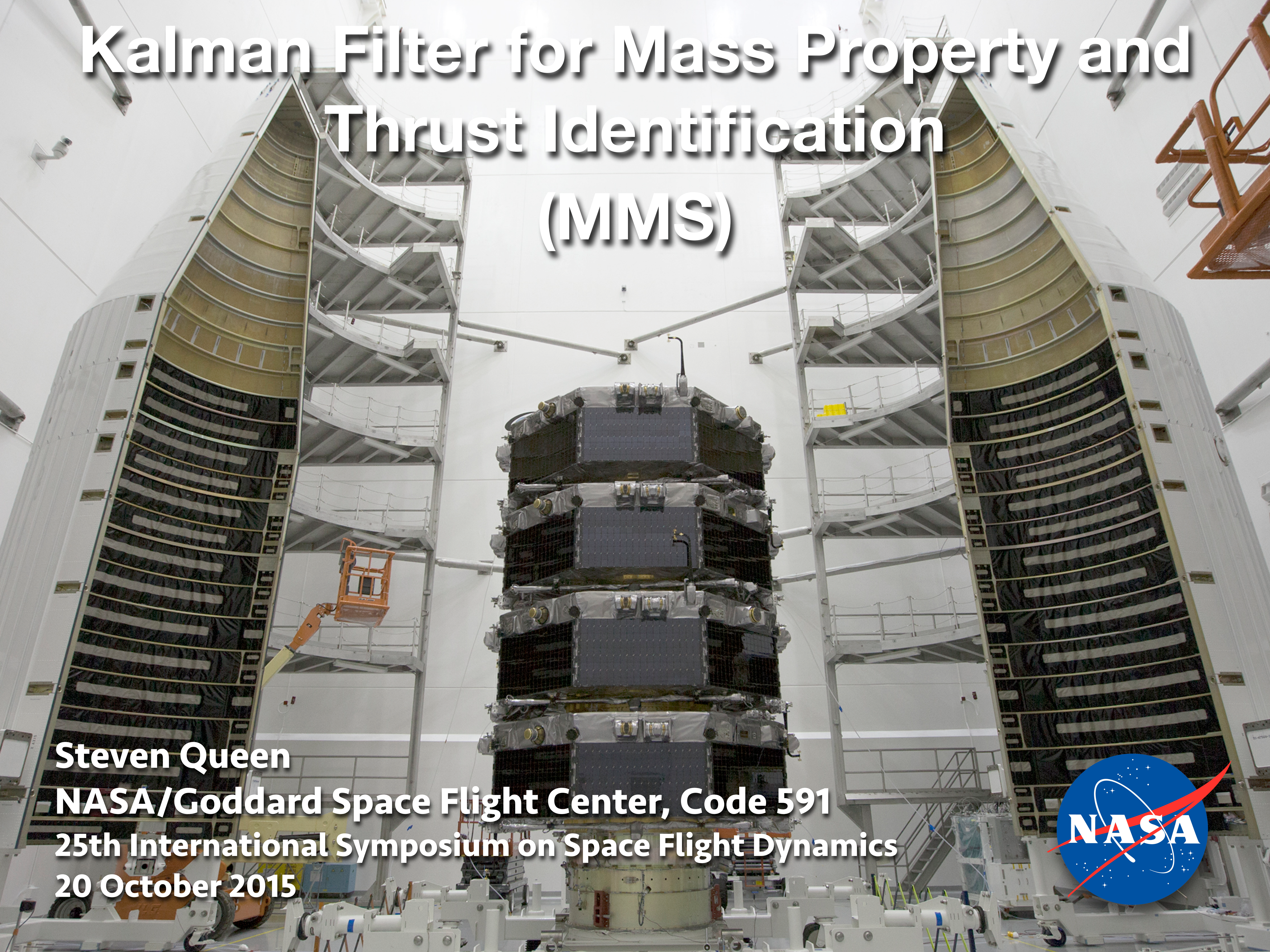

Kalman Filter for Mass Property and Thrust Identification (MMS)

Steven Queen

NASA/Goddard Space Flight Center, Code 591

25th International Symposium on Space Flight Dynamics

20 October 2015

Topics Covered

Multiplicative Extended Kalman Filter (MEKF) for MMS On–board Attitude and Rate Determination

- MEKF formulation (points-of-interest)
- Measurement Model (star sensor)
- Flight Performance

MEKF for Identification of System Properties

(center-of-mass, moments of inertia, and thrust)

- State Augmentation
- Measurement Model (accelerometer)
- Thruster Warm-Up Model
- Simulated Test-Case Performance
- Simulated Monte Carlo Performance
- Flight Performance

Brief MEKF Review

Multiplicative Extended Kalman Filter

- Extended Kalman Filter (EKF) variant
- 1st flight use SPARS (1969)
- rigorous formation by Lefferts, Markley, and Shuster (1982)
- continued refinement and advocacy by Markley (2003)

EKF with Additive Update

$$\mathbf{q}_{\text{true}} = \Delta\mathbf{q} + \hat{\mathbf{q}}$$

error quaternion state used in filter

full (global) state estimate

✗ Unity Norm
✗ Unbiased

MEKF Multiplicative Update

$$\mathbf{q}_{\text{true}} = \delta\mathbf{q}^{\otimes}\hat{\mathbf{q}}$$

error quaternion **not** directly used in filter

full (global) state estimate

✓ Unity Norm
✓ Unbiased

Quaternion Left-Multiple Operator

$$\mathbf{q}^{\otimes} \equiv \begin{bmatrix} q_1 \\ q_2 \\ q_3 \\ q_4 \end{bmatrix}^{\otimes} = \begin{bmatrix} \mathbf{q}_{1:3} \\ q_4 \end{bmatrix}^{\otimes} = q_4 \mathbb{I}_4 + \begin{bmatrix} -\mathbf{q}_{1:3}^{\times} & \mathbf{q}_{1:3} \\ -\mathbf{q}_{1:3}^{\mathsf{T}} & 0 \end{bmatrix} = \begin{bmatrix} q_4 \mathbb{I}_3 - \mathbf{q}_{1:3}^{\times} & \mathbf{q}_{1:3} \\ -\mathbf{q}_{1:3}^{\mathsf{T}} & q_4 \end{bmatrix}$$

Skew-Symmetric "Cross-Product" Operator

$$\boldsymbol{\omega}^{\times} \equiv \begin{bmatrix} \omega_x \\ \omega_y \\ \omega_z \end{bmatrix}^{\times} = \begin{bmatrix} 0 & -\omega_z & \omega_y \\ \omega_z & 0 & -\omega_x \\ -\omega_y & \omega_x & 0 \end{bmatrix}$$

MEKF Error State Idiosyncrasies

The MEKF uses a reduced three component attitude parameterization as the error-state inside the filter.

- Could use any three-component attitude representation (e.g. Euler rotation axis/angle, Gibbs vector, Modified Rodrigues parameters, Tait-Bryan angles, etc.)
- MMS chose (twice) the Gibbs vector parameterization:
  - free of singularities up to ±180°
  - largest possible 180° map to infinity (compatible with Gaussian "tails")
  - avoids accumulation of numerical errors in full-state quaternion norm through explicit normalization in *reset operation* that is neither *ad hoc* or require transcendental evaluations
  - observation model insensitive to sign ambiguity in star camera's output quaternion
  - diagonals of error covariance matrix (P) map directly to attitude error variance (σ^2)

mappings

$$\underbrace{\boldsymbol{\delta\theta}}_{\text{error state used in filter}} \equiv \underbrace{2\boldsymbol{\delta}\mathbf{g}}_{\text{Gibbs vector attitude error}} \equiv \underbrace{2\,\frac{\delta\mathbf{q}_{1:3}}{\delta q_4}}_{\text{relationship to error quaternion}}$$

inverse mappings

$$\boldsymbol{\delta}\mathbf{q} = \frac{\pm 1}{\sqrt{1+\|\boldsymbol{\delta}\mathbf{g}\|^2}}\begin{bmatrix}\boldsymbol{\delta}\mathbf{g}\\ 1\end{bmatrix} = \frac{1}{\sqrt{4+\|\boldsymbol{\delta\theta}\|^2}}\begin{bmatrix}\boldsymbol{\delta\theta}\\ 2\end{bmatrix} \approx \begin{bmatrix}\dfrac{\boldsymbol{\delta\theta}}{2}\\ 1\end{bmatrix}$$

(1st order only)

On-board MEKF Models

State Dynamics

Nonlinear Full-State Model	Linearized Error-State Model
$\dot{\mathbf{x}}(t) = \mathbf{f}(\mathbf{q}(t), \boldsymbol{\omega}(t), \mathbf{u}(t), \mathbf{w}(t)) = \begin{Bmatrix} \mathbf{f}_q(\mathbf{q}, \boldsymbol{\omega}) \\ \mathbf{f}_\omega(\boldsymbol{\omega}, \mathbf{u}) \end{Bmatrix} + G\mathbf{w}$ $\begin{Bmatrix} \dot{\mathbf{q}} \\ \dot{\boldsymbol{\omega}} \end{Bmatrix} = \begin{Bmatrix} \frac{1}{2}\begin{bmatrix} -\boldsymbol{\omega}^\times & \boldsymbol{\omega} \\ -\boldsymbol{\omega}^\mathsf{T} & 0 \end{bmatrix}\mathbf{q} \\ \mathbf{I}^{-1}\left[\boldsymbol{\tau}(\mathbf{u}) - \boldsymbol{\omega}^\times \mathbf{I}\boldsymbol{\omega}\right] \end{Bmatrix} + G\mathbf{w}$	$\delta\dot{\mathbf{x}} = \mathbf{f}(\delta\boldsymbol{\theta}(t), \delta\boldsymbol{\omega}(t), \mathbf{u}(t), \mathbf{w}(t)) = \begin{Bmatrix} \mathbf{f}_\theta(\delta\boldsymbol{\theta}, \delta\boldsymbol{\omega}) \\ \mathbf{f}_\omega(\delta\boldsymbol{\omega}, \mathbf{u}) \end{Bmatrix} + G(t)\mathbf{w}$ $\begin{bmatrix} \delta\dot{\boldsymbol{\theta}} \\ \delta\dot{\boldsymbol{\omega}} \end{bmatrix} \approx \begin{bmatrix} -\hat{\boldsymbol{\omega}}^\times & \mathbb{I}_3 \\ \mathbf{0}_{3\times 3} & \mathbf{I}^{-1}\left[(\mathbf{I}\hat{\boldsymbol{\omega}})^\times - \hat{\boldsymbol{\omega}}^\times \mathbf{I}\right] \end{bmatrix} \begin{bmatrix} \delta\boldsymbol{\theta} \\ \delta\boldsymbol{\omega} \end{bmatrix} + \begin{bmatrix} \mathbf{w}_\theta \\ \mathbf{w}_\omega \end{bmatrix} \approx F(t)\,\delta\mathbf{x} + \mathbf{w}$
Process Noise: $\mathbf{w}(t) \sim N(\mathbf{0}, Q(t))$	

MMS has no gyros.
Inertia matrix knowledge is required.

Derivation of attitude error dynamics derivation a bit more involved than for non-additive states.

Measurement Updates

$$\begin{bmatrix} \delta\boldsymbol{\theta}_k^+ \\ \delta\boldsymbol{\omega}_k^+ \end{bmatrix} = \underbrace{\cancel{\begin{bmatrix} \delta\boldsymbol{\theta}_k^- \\ \delta\boldsymbol{\omega}_k^- \end{bmatrix}}}_{\text{zero due to reset op}} + \underbrace{K_k}_{\text{"standard" Kalman gain}} \overbrace{\left\{ \underbrace{\mathbf{y}_k}_{\text{measurement}} - \underbrace{\mathbf{h}\left(\hat{\mathbf{q}}_k^-, \hat{\boldsymbol{\omega}}_k^-\right)}_{\text{expected measurement (based on full-state est.)}} - \underbrace{H_k\left(\hat{\mathbf{q}}_k^-, \hat{\boldsymbol{\omega}}_k^-\right)}_{\text{(linearize) measurement sensitivity matrix}} \underbrace{\cancel{\begin{bmatrix} \delta\boldsymbol{\theta}_k^- \\ \delta\boldsymbol{\omega}_k^- \end{bmatrix}}}_{\text{zero due to reset op}} \right\}}^{\text{measurement residual } \boldsymbol{\rho}_k}$$

$$H_k \equiv \left[\frac{\partial \mathbf{h}}{\partial \mathbf{q}} \cdot \frac{\partial \mathbf{q}}{\partial(\delta\boldsymbol{\theta})} \quad \frac{\partial \mathbf{h}}{\partial \boldsymbol{\omega}} \right]_{\hat{\mathbf{q}}_k, \hat{\boldsymbol{\omega}}}$$

Even though H_k is not used here (due to *reset op*) it is needed for covariance propagation. NOTE: partial derivatives are with respect to error states (but result only differs for non-additive states).

Star Sensor

µASC Star Tracker System (STS) provided by the Technical University of Denmark (DTU)

- Four camera head units (CHUs)
- Redundant centralized electronics
- 4 Hz update rate
- Measurements combined as a pre-processing step in to single measurement update for computationally simpler on-board MEKF processing
- Spec performance levels (4 heads combined):

Axis	Accuracy (1σ)
Transverse	20 arcsec
Boresite	60 arcsec

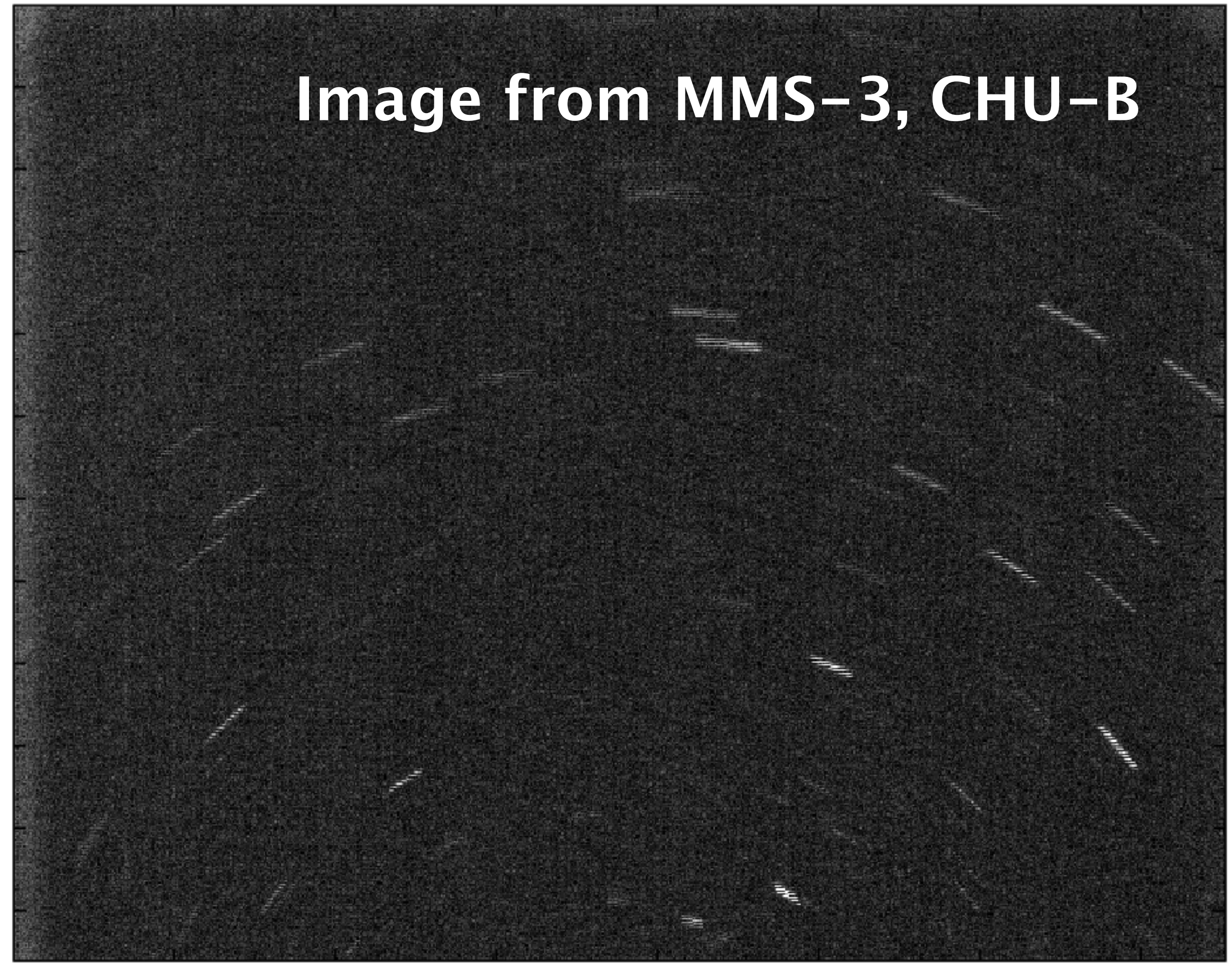

Measurement Model

$$(\mathbf{y}_{\text{chu}})_k = (\mathbf{h}_{\text{chu}})_k = \boldsymbol{\delta\theta}_k + (\mathbf{v}_{\text{chu}})_k = (\boldsymbol{\delta\theta}_{\text{chu}})_k = 2\frac{(\boldsymbol{\delta}\mathbf{q}_{1:3})_k}{(\delta q_4)_k} = 2\frac{\left((\mathbf{q}_{\text{chu}})_k^{\otimes}\,\hat{\mathbf{q}}_k^{-1}\right)_{1:3}}{\left((\mathbf{q}_{\text{chu}})_k^{\otimes}\,\hat{\mathbf{q}}_k^{-1}\right)_4}$$

Insensitive to STS quaternion sign!

Measurement Residual

$$(\boldsymbol{\rho}_{\text{chu}})_k = (\mathbf{y}_{\text{chu}})_k - \mathbf{h}\left(\hat{\mathbf{q}}_k^-, \hat{\boldsymbol{\omega}}_k^-\right) - H_{\text{chu}}\begin{bmatrix}\boldsymbol{\delta\theta}_k^- \\ \boldsymbol{\delta\omega}_k^-\end{bmatrix} = (\boldsymbol{\delta\theta}_{\text{chu}})_k$$

zero

zero due to *reset op*

$$\boxed{H_{\text{chu}} = \left[\frac{\partial \mathbf{h}_{\text{chu}}}{\partial(\boldsymbol{\delta\theta})} \quad \frac{\partial \mathbf{h}_{\text{chu}}}{\partial \boldsymbol{\omega}}\right]_{\hat{\mathbf{q}}_k, \hat{\boldsymbol{\omega}}} = \left[\mathbb{I}_3 \quad \mathbf{0}_{3\times 3}\right]}$$

On-orbit Performance

Examining the performance of the MEKF rate estimation for the first two thruster-pulses of a calibration maneuver (EA019) executed on 1 April 2015.

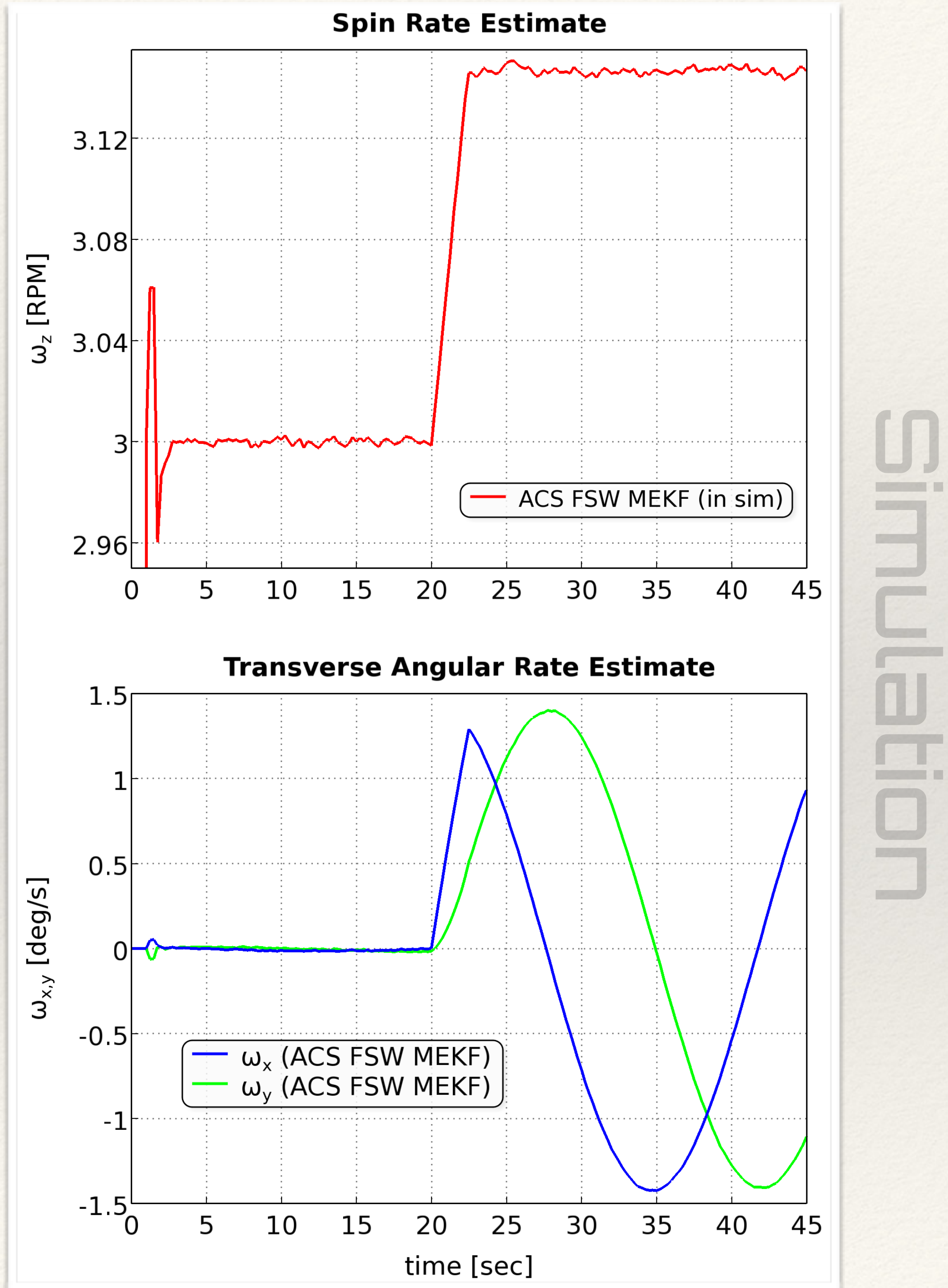

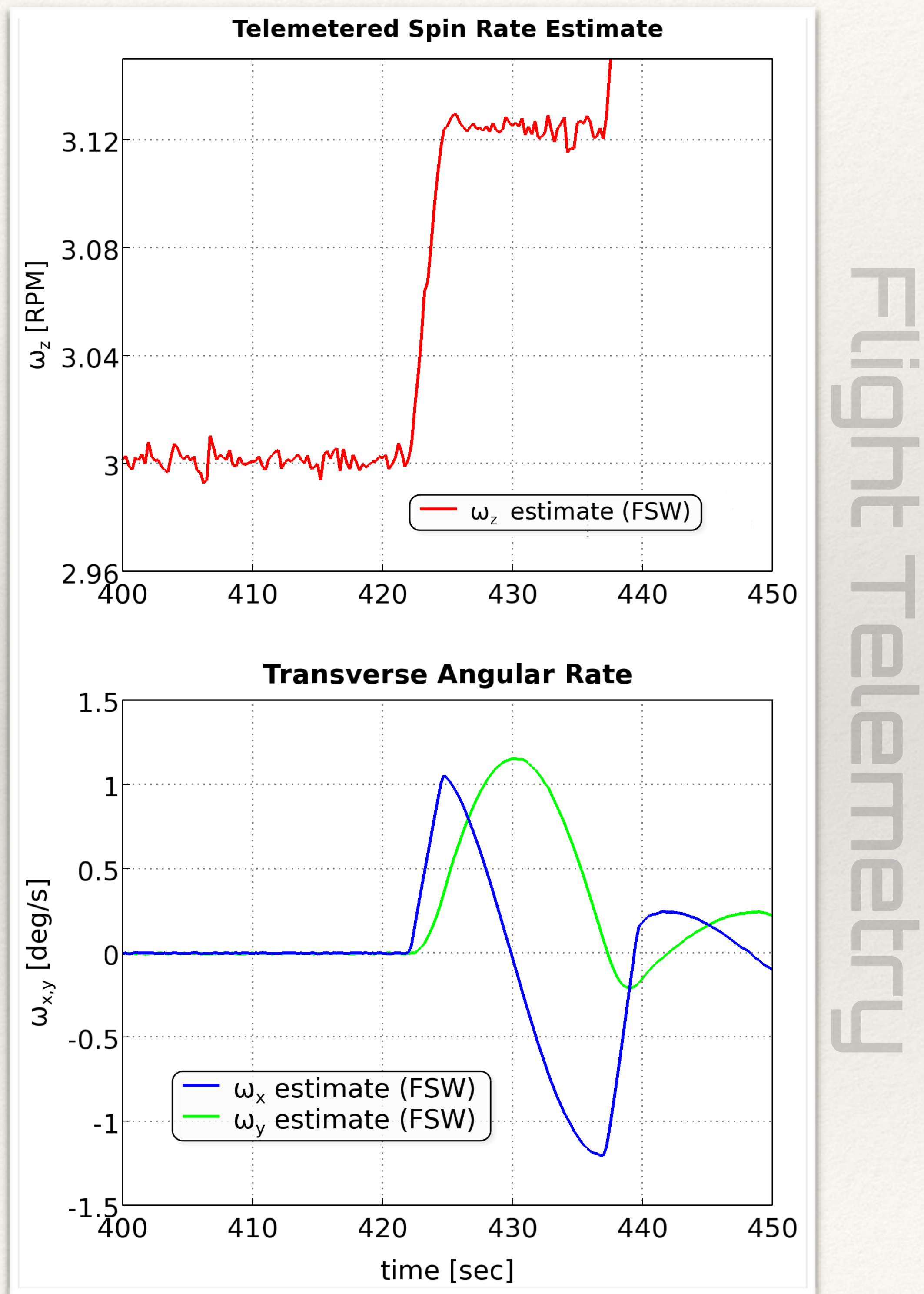

Full Calibration Maneuver

Full EA019 maneuver rate profile

- exercises all twelve thrusters individually, in matched pulse-pairs, 1/2 nutation cycle apart
- thrusters #1 (radial) and #12 (axial) exercised in double pairs to characterize warm-up

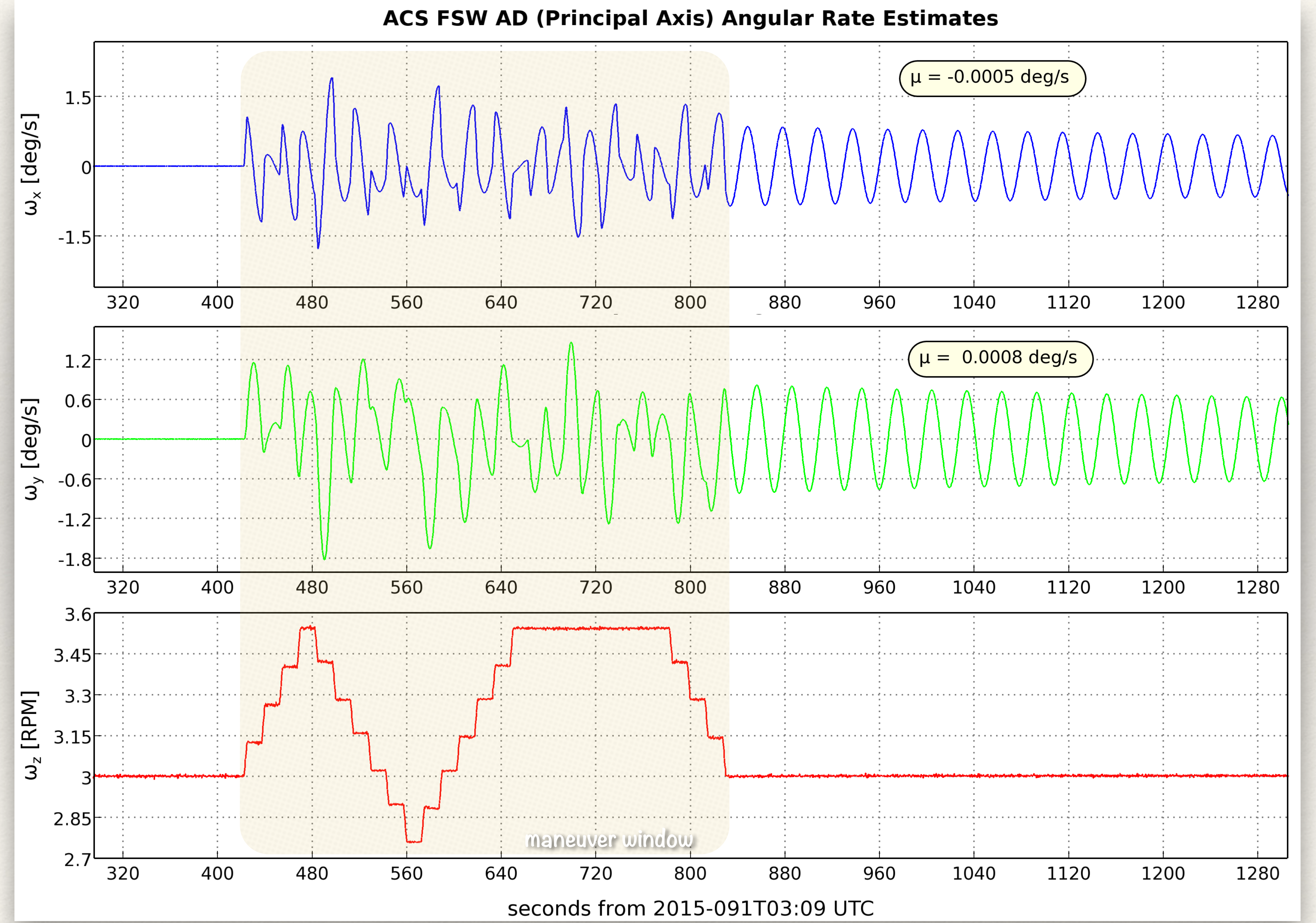

Flight Telemetry

EA019 STS Measurement Residuals

Star Tracker per Camera Head Unit (CHU) Measurement Residuals

Axis	Spec* (1σ)
Transverse	20 asec
Boresite	60 asec

*expected ensemble solution performance with all four heads measurements

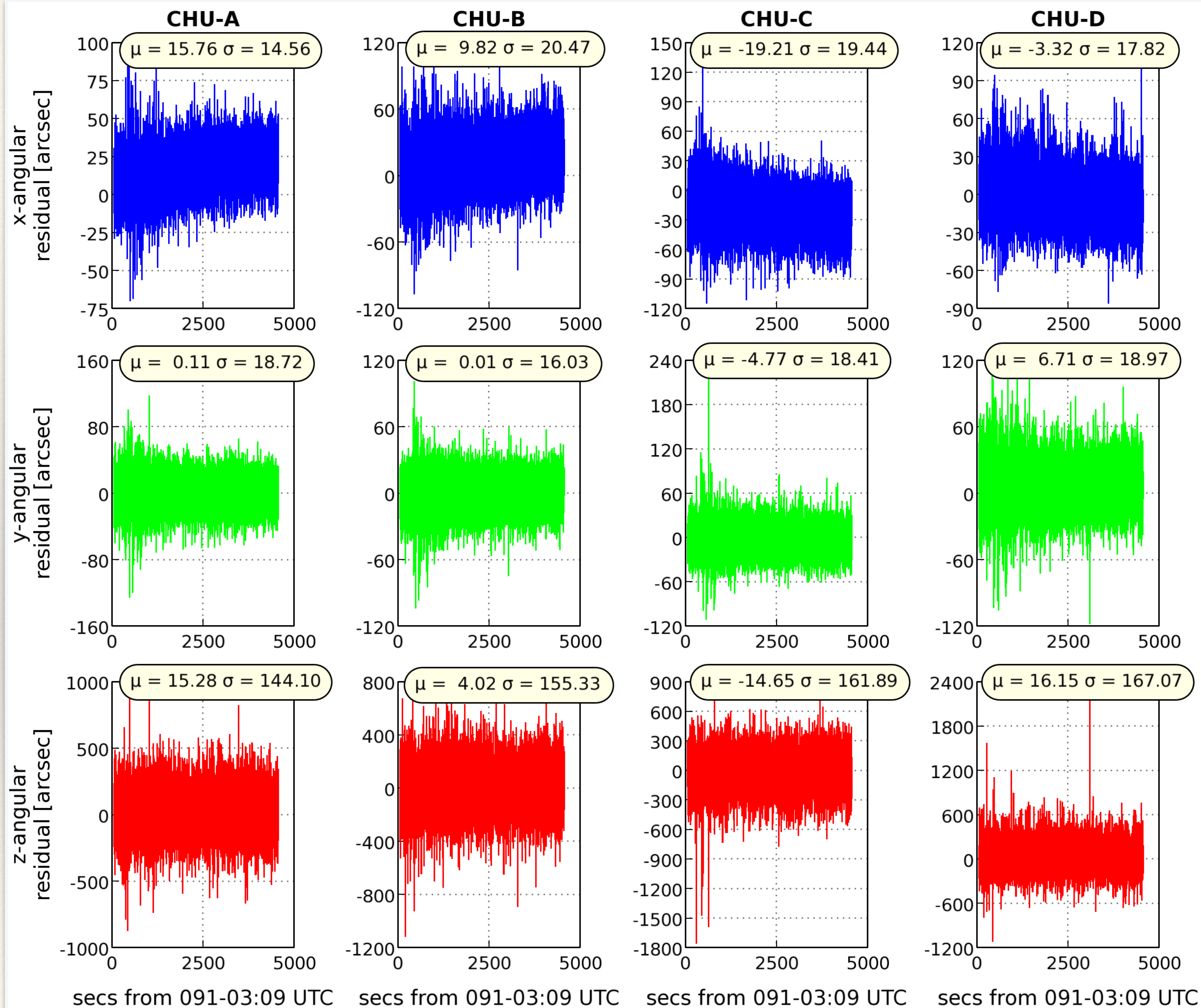

Flight Telemetry

Augmented MEKF for Ground-based System Identification

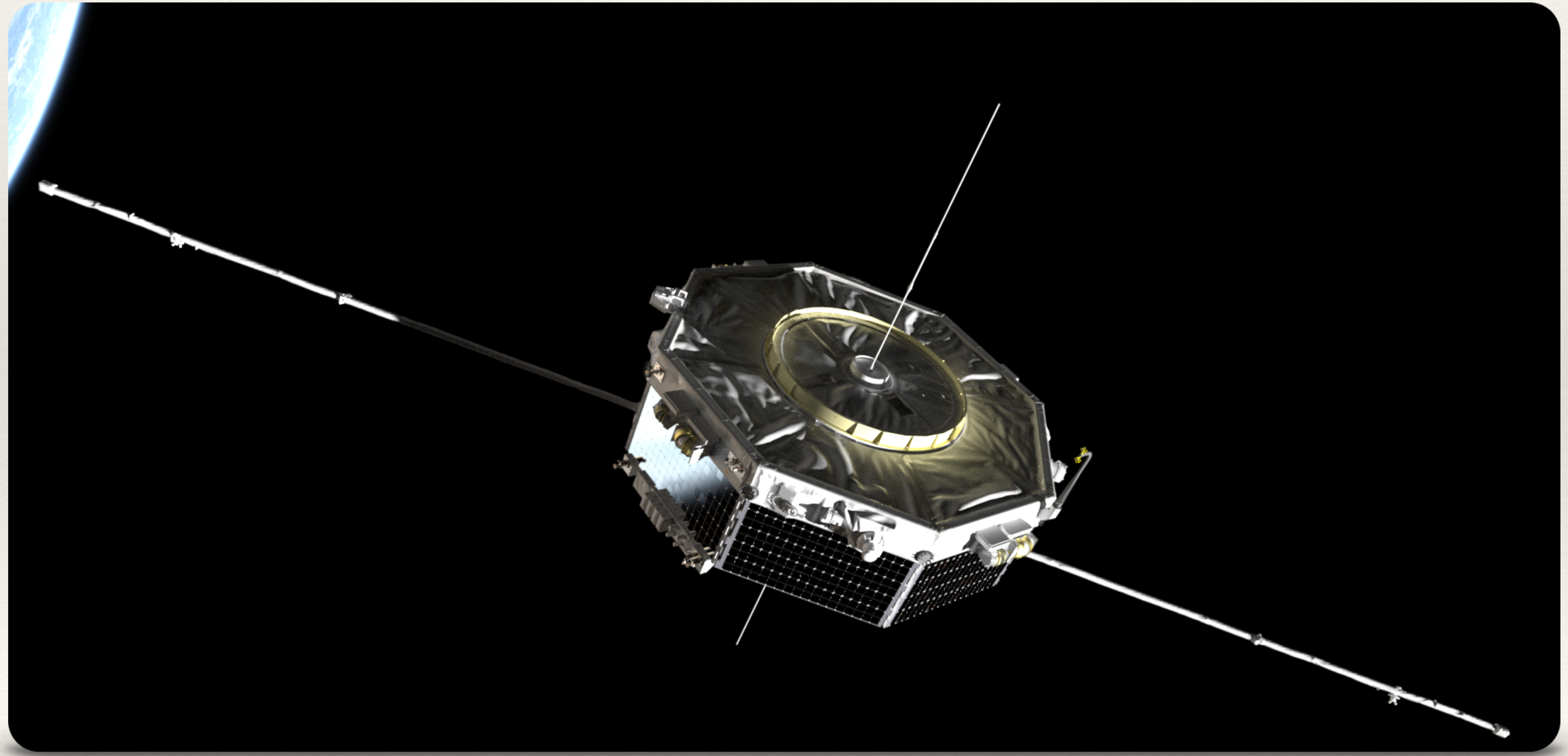

Case for System ID State Augmentation

MMS maneuvering performance requires accurate knowledge of

- **(Fuel) Inertia Tensor**—lacking gyroscopes, the second mass moment of inertia knowledge directly affects the accuracy of the rate estimate. Angular rate errors (along with center-of-mass knowledge) affect the centripetal compensation algorithms used in closed-loop orbital maneuvers. *Since the dry system properties were well known prior to launch, only the fuel's contribution to inertia is estimated.*
- **(Fuel) Center-of-Mass**—knowledge of the lever-arm from the CM to the accelerometer sensor heads affects the ability to remove gyro-dynamic biases from the incremental velocity output of the AMS.
- **Steady-State Thrust—**closed-loop incremental velocity feedback removes the majority of the maneuvering system's sensitivity to knowledge errors in thruster. However, in order to achieve 1% (3σ) maneuvering accuracy, it was shown via Monte Carlo simulations that 3% (3σ) steady-state thrust knowledge was necessary due to the corruption of rate-propagation with an incorrect torque (gyro rate-substitution would alleviate).
- **Warm-up Knock-down Factor**—warm-up effects of the cat-bed in the hydrazine thruster's thrust-chamber can degrade initial thrust by as much as 15%. In order to account for this in the system dynamics, a simplified thermal-model of the thruster was added to the MEKF. Two thermal-states per thruster are required. Thermal coefficients of the model were determined from pre-flight test data.
- **Accelerometer Intrinsic Biases**—in order to use the accelerometer measures for thrust-determination, the intrinsic thermo-electrical biases of the AMS sensor heads must also be estimated.

Augmented State Vector

$$\delta\mathbf{x} = \big[\underbrace{\boldsymbol{\delta\theta} \quad \boldsymbol{\delta\omega}}_{\text{original FSW states}} \quad \underbrace{\boldsymbol{\delta}\mathbf{b}}_{\text{AMS biases}} \quad \underbrace{\boldsymbol{\delta}\mathbf{r}_{\mathsf{f}}}_{\text{fuel CM}} \quad \underbrace{\boldsymbol{\delta}\mathbf{I}_{\mathsf{f}}}_{\substack{\text{fuel inertia} \\ \text{6 states vector}}} \quad \underbrace{\boldsymbol{\delta}\mathrm{f}_{ss}}_{\text{steady-state thrust}} \quad \underbrace{\boldsymbol{\delta}\mathrm{T}_{c}}_{\text{thrust chamber temp}} \quad \underbrace{\boldsymbol{\delta}\mathrm{T}_{x}}_{\text{structure temp}}\big]^{\mathsf{T}}$$

Acceleration Measurement System

Acceleration Measurement System (AMS), manufactured by ZIN Technologies

- three orthogonal Honeywell QA3000 accelerometers
- 100 kHz analog-to-digital sampling
- dynamic range of greater than ±25,000 μg
- resolution of less than 1 μg
- short-term (1σ) bias stability over a twelve hour period of better than 1 μg
- effective bandwidth of 250 Hz
- 1 KHz (down-sampled) acceleration integrated (corrected and summed) to produce an incremental velocity-change output at 4 Hz
- low-pass bias estimation filter

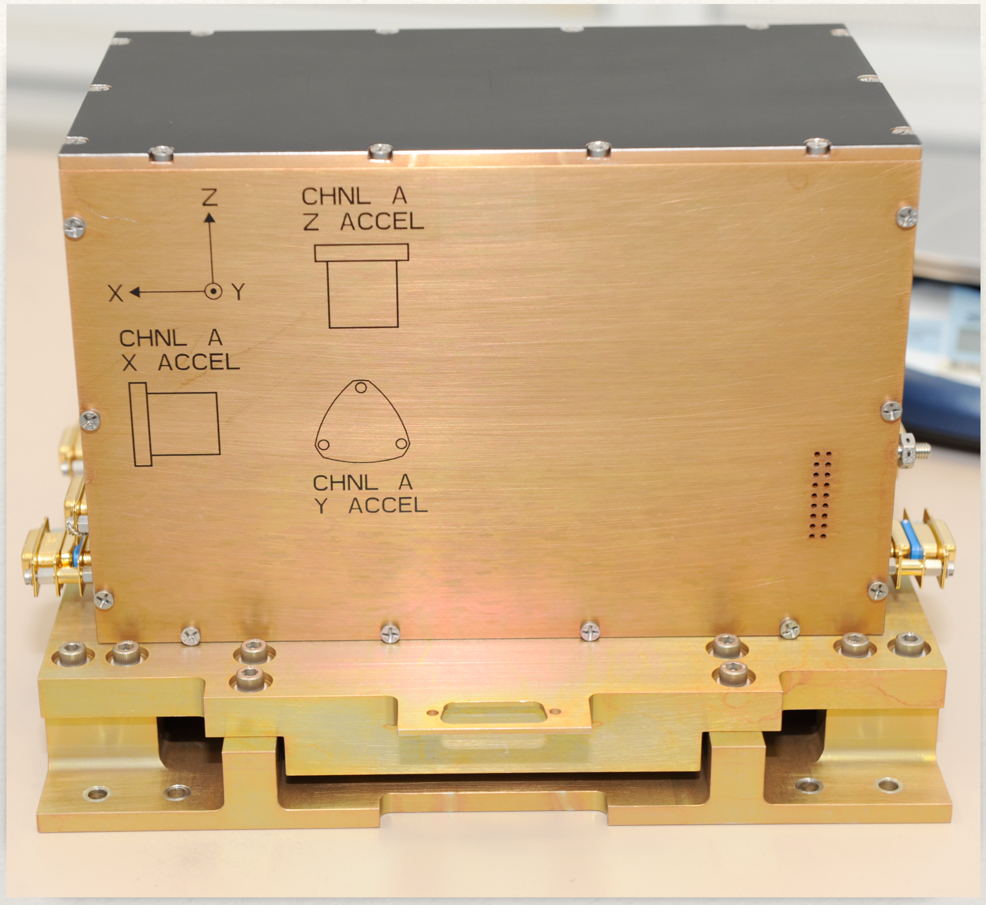

Accelerometer Measurement Model

Modeled as a proof-mass connected to a rigid-body by tri-axial springs, the device acceleration relative to a body-fixed origin is

$$\mathbf{a}_d \equiv -\frac{k_d}{m_p}\boldsymbol{\xi} = \underset{b\leftarrow i}{\mathcal{A}}\left(\dot{\mathbf{V}}_o - \mathbf{a}_{\mathsf{grav}}\right) + \dot{\boldsymbol{\omega}}^\times \mathbf{r}_d + \boldsymbol{\omega}^\times\boldsymbol{\omega}^\times\mathbf{r}_d$$

Introducing the base-body's center-of mass ($\mathbf{r}_c$) yields a truth model

$$\mathbf{a}_d = \frac{\mathbf{f}_{\mathsf{t}}}{m} + \dot{\boldsymbol{\omega}}^\times \underbrace{(\mathbf{r}_d - \mathbf{r}_c)}_{\mathbf{r}_{cd}} + \boldsymbol{\omega}^\times\boldsymbol{\omega}^\times (\mathbf{r}_d - \mathbf{r}_c) - \underbrace{\left(2\cdot\boldsymbol{\omega}^\times\dot{\mathbf{r}}_c + \ddot{\mathbf{r}}_c\right)}_{\text{multi-body effects}}$$

where $\mathbf{f}_{\mathsf{t}}$ is the acceleration due to body-fixed thrusters.

Acceleration measurement model assumes n uni-axial measurements (along $\mathbf{u}_n$) corrupted by bias, noise and scale factor errors

$(\mathsf{h}_{\mathsf{ams}})_k$

$$\mathbf{a}_k = \begin{bmatrix} a_x \\ a_y \\ a_z \end{bmatrix}_{t_k} = \underbrace{\left(\mathcal{O}^{\mathsf{T}}\mathcal{O}\right)^{-1}\mathcal{O}^{\mathsf{T}}}_{\substack{\text{pseudo}-\text{inverse} \\ \text{of orthogonality matrix}}} \left\{ \begin{bmatrix} (1+\delta\kappa_1)\,\hat{\mathbf{u}}_1^{\mathsf{T}} \\ (1+\delta\kappa_2)\,\hat{\mathbf{u}}_2^{\mathsf{T}} \\ \vdots \\ (1+\delta\kappa_n)\,\hat{\mathbf{u}}_n^{\mathsf{T}} \end{bmatrix} \mathbf{a}_d + \underbrace{\begin{bmatrix} b_1 \\ b_2 \\ \vdots \\ b_n \end{bmatrix}}_{\text{bias}} + \underbrace{\begin{bmatrix} \eta_1 \\ \eta_2 \\ \vdots \\ \eta_n \end{bmatrix}}_{\text{noise}} \right\}$$

scale factor | sensing direction

Augmented Measurement Models

STS measurement sensitivity matrix

$$(H_{\mathsf{chu}})_k = \begin{bmatrix} \mathbb{I}_3 & \mathbf{0}_{3\times3} & \mathbf{0}_{3\times3} & \mathbf{0}_{3\times3} & \mathbf{0}_{3\times3} & \mathbf{0}_{3\times3} & \mathbf{0}_{3\times3} & \mathbf{0}_{3\times3} \end{bmatrix}_{\hat{\mathbf{x}}_k}$$

AMS measurement sensitivity matrix

$$(H_{\mathsf{ams}})_k = \begin{bmatrix} \mathbf{0}_{3\times3} & \dfrac{\partial \mathbf{h}_{\mathsf{ams}}}{\partial \boldsymbol{\omega}} & \mathbb{I}_3 & \dfrac{\partial \mathbf{h}_{\mathsf{ams}}}{\partial \mathbf{r}_{\mathsf{f}}} & \dfrac{\partial \mathbf{h}_{\mathsf{ams}}}{\partial \mathbf{I}_{\mathsf{f}}} & \dfrac{\partial \mathbf{h}_{\mathsf{ams}}}{\partial \mathrm{f}_{ss}} & \dfrac{\partial \mathbf{h}_{\mathsf{ams}}}{\partial \mathrm{T}_c} & \mathbf{0}_{3\times3} \end{bmatrix}_{\hat{\mathbf{x}}_k}$$

AMS measurement noise

$$A_{0-10\,\mathsf{hz}} \leq \frac{(a_{\mathsf{rms}})^2}{\Delta f_{\mathsf{hz}}} = \frac{8^2\,\mu g^2}{10\,\mathrm{Hz}} = 6.4\,\frac{\mu g^2}{\mathrm{Hz}} = 615.9\frac{\left(\frac{\mu\mathrm{m}}{\mathrm{s}^2}\right)^2}{\mathrm{Hz}}$$

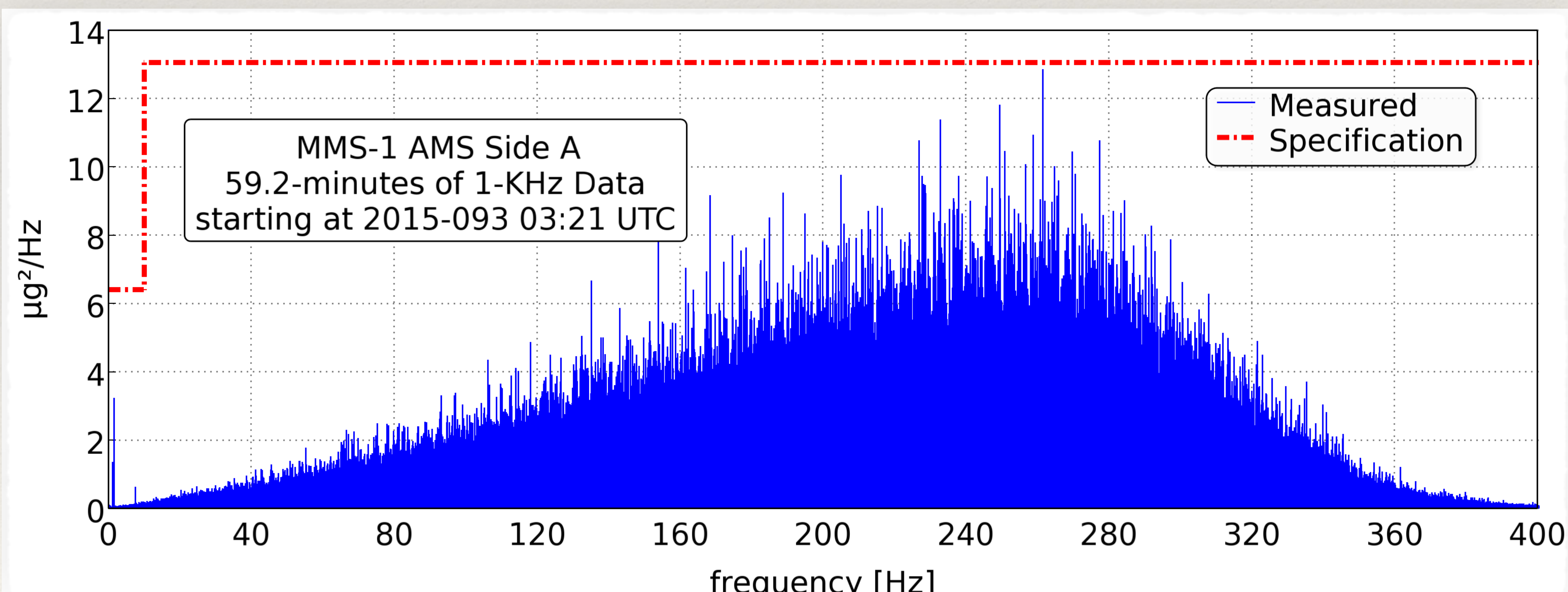

System ID: 2-Pulse Test-Case

Introduced knowledge errors into a simulated test-case system

- pair of pulses from thruster #1 at 20 and 36 secs

Parameter	Error
accelerometer biases	$+20\ \mu g$
fuel center-of-mass	$+50$ mm
fuel moments of inertia	$+10$ kg-m^2
steady-state thrust magnitude	$+5\%$

Steady-State Force Estimation Test-Case Results

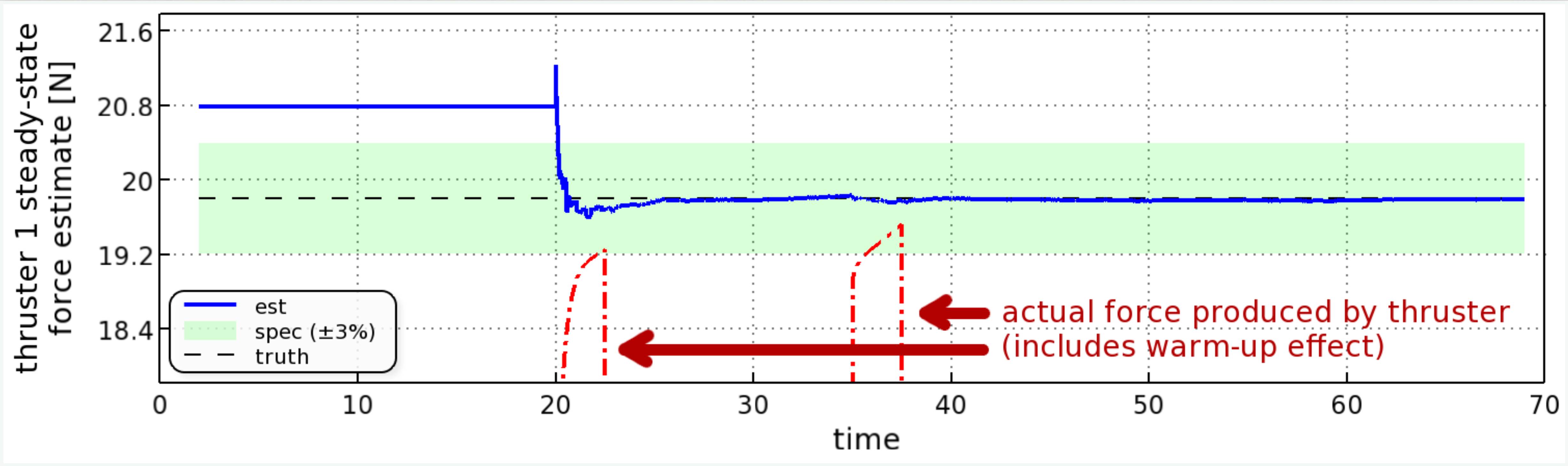

System ID: 2-Pulse Test-Case

Composite Center-of-Mass Estimation Test-Case Results

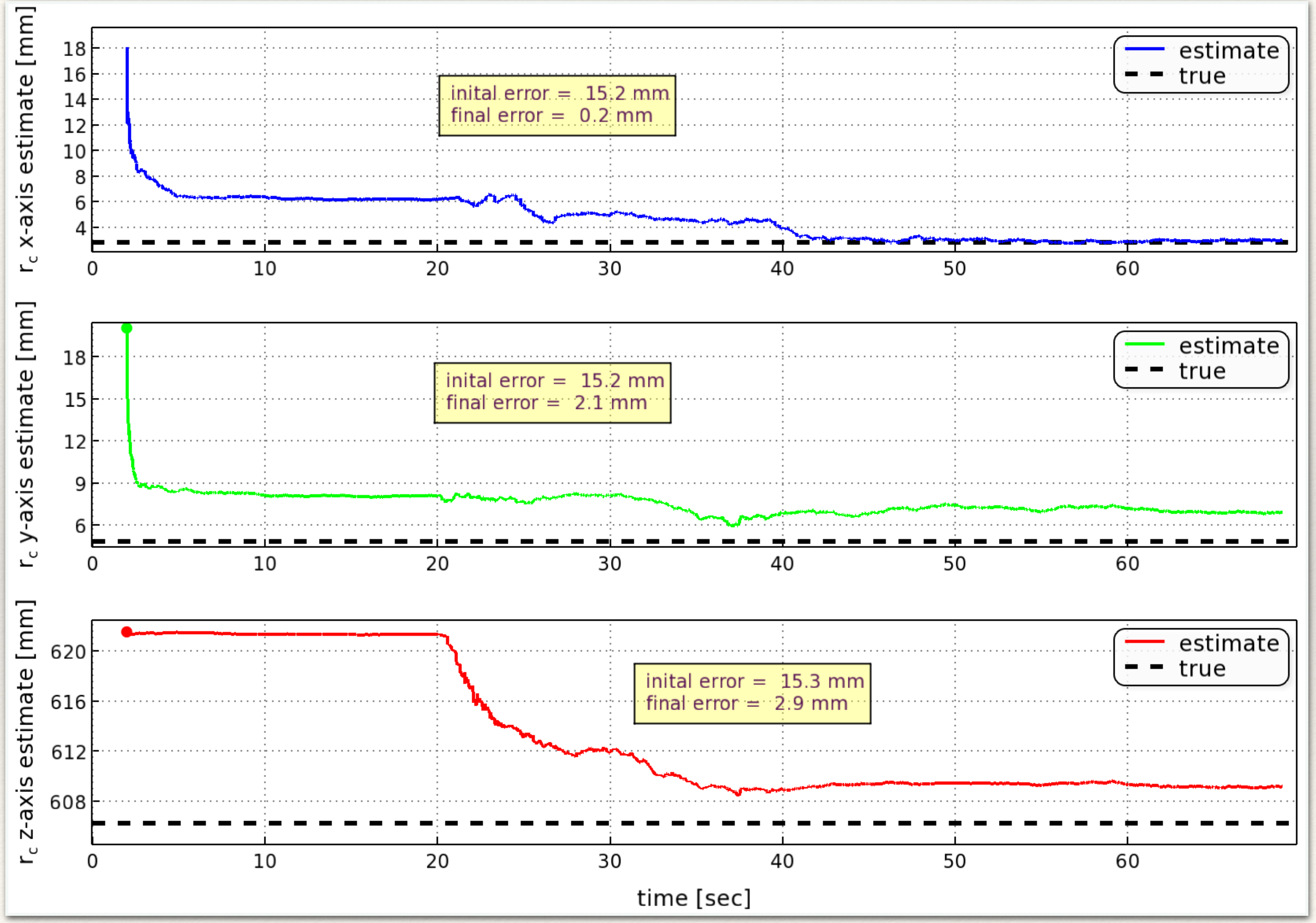

System ID: 2-Pulse Test-Case

Composite Inertia Tensor
Estimation Test-Case Results

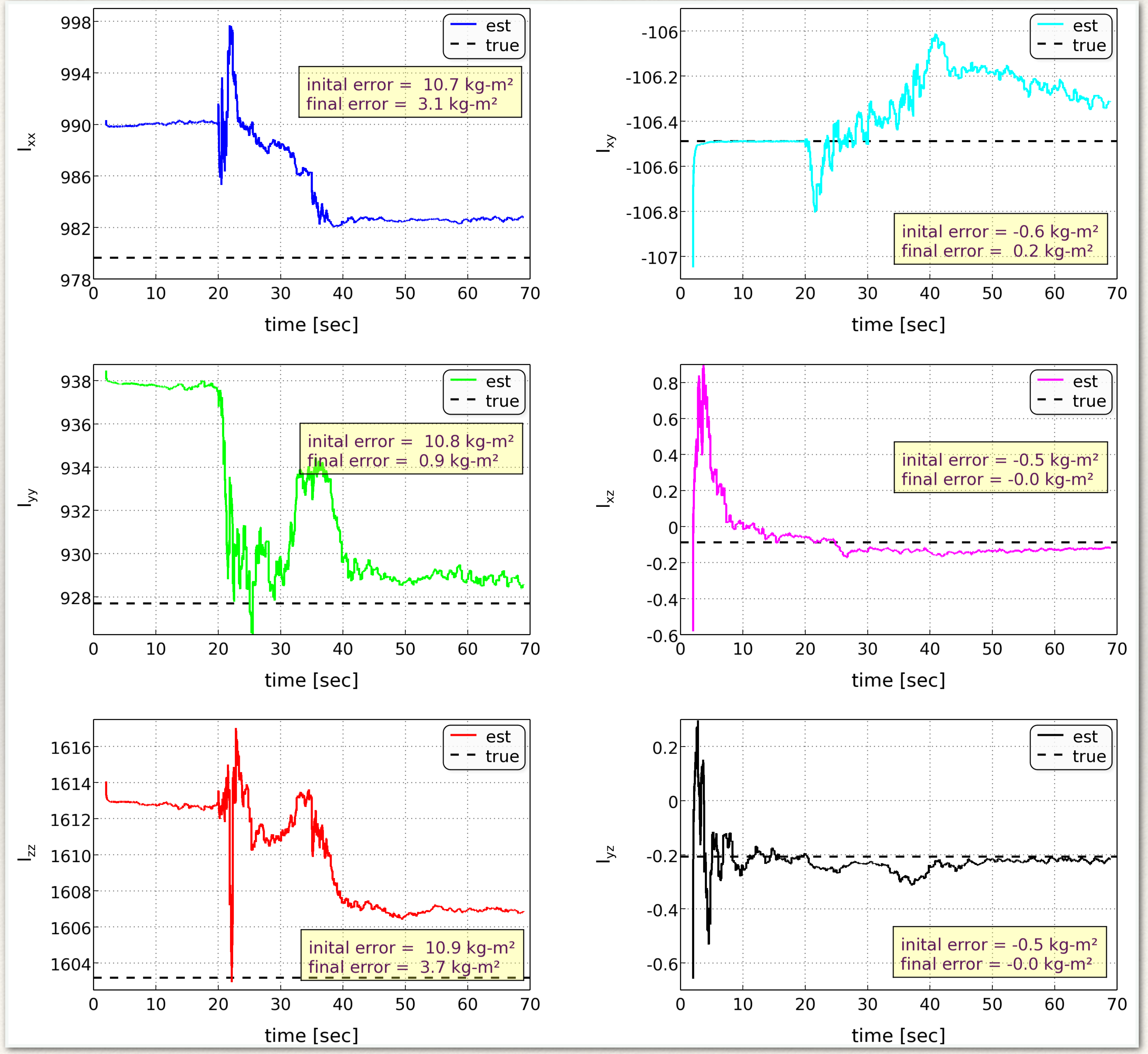

System ID: 2-Pulse Test-Case

AMS Bias Estimation Test-Case Results

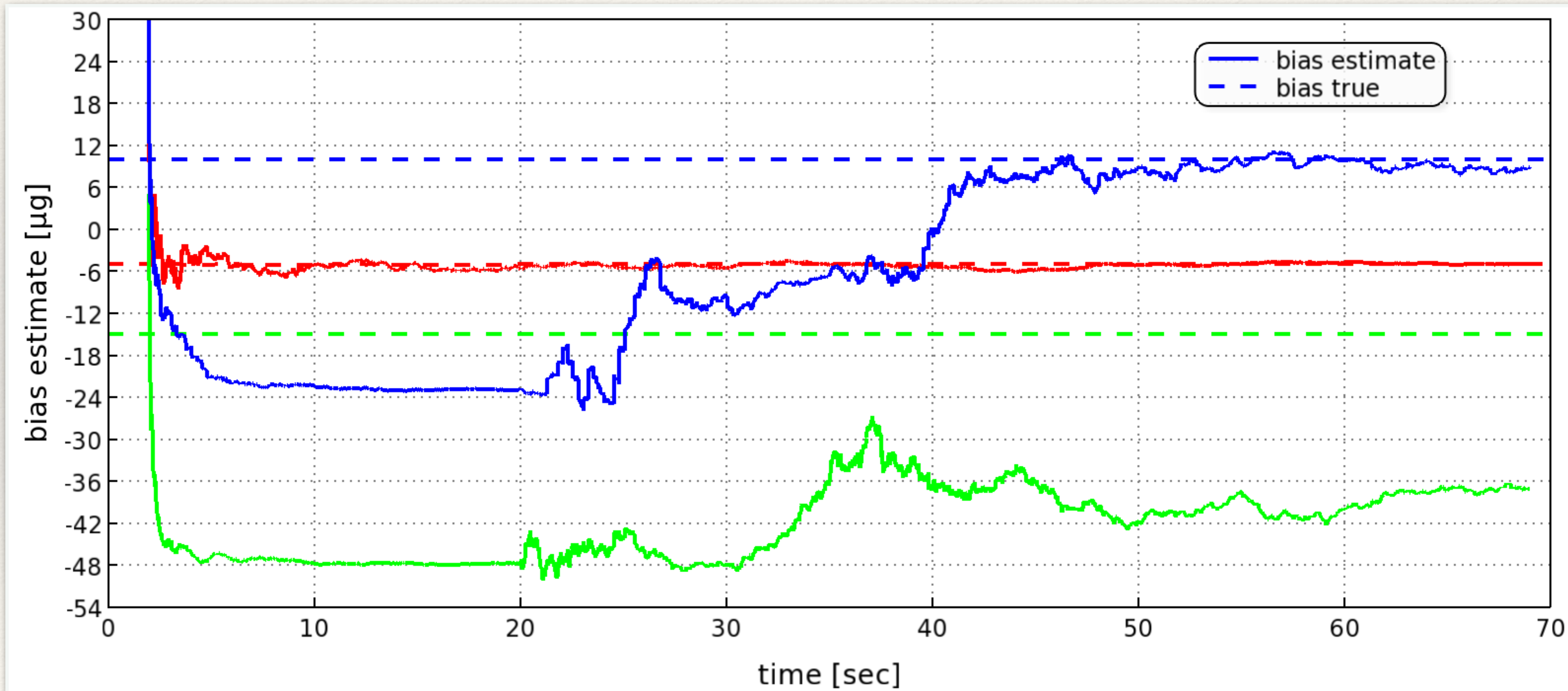

System ID: Monte Carlo Results

Hundreds of parameters in the high-fidelity simulation of the MMS spacecraft were randomly perturbed within the expected distributions and (conservative) uncertainty limits of ground-based knowledge.

The full EA019 maneuver was simulated and statistics collected on the accuracy of the augmented MEKF system identification process. The results from 300 runs are shown.

Steady-State Thrust Estimation Monte Carlo Statistics

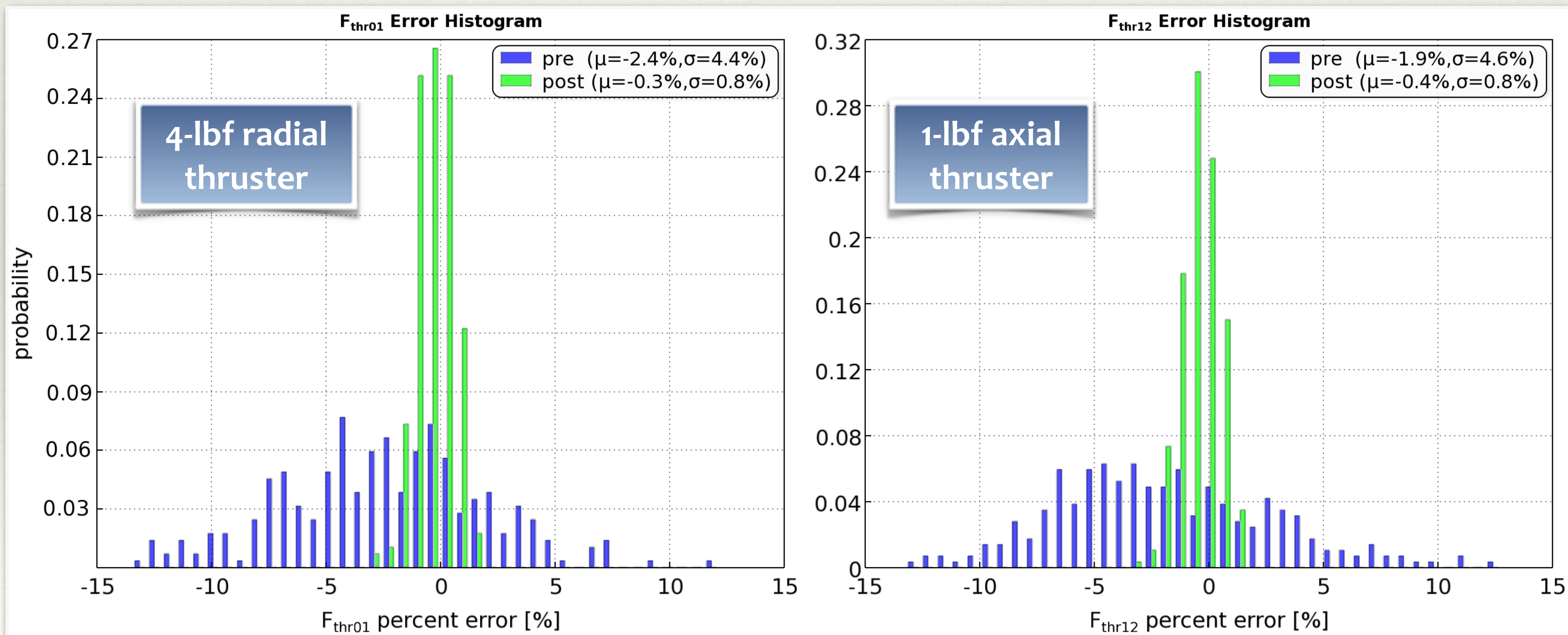

System ID: Monte Carlo Results

Composite Mass Property Estimation Monte Carlo Statistics

Center of Mass

Moments of Inertia

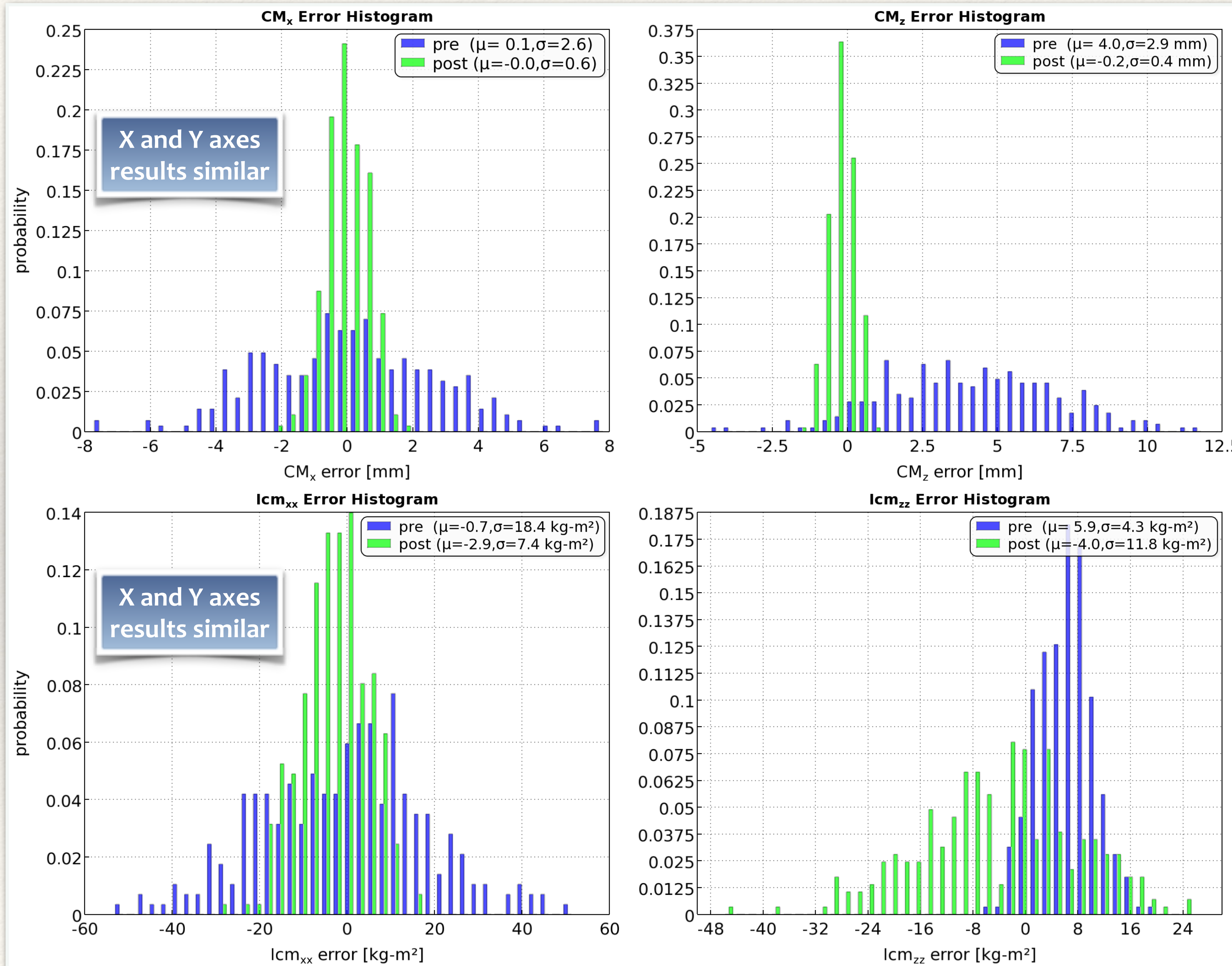

System ID: MMS1 EA019 Flight Results

Ground processing of the EA019 maneuver for MMS1 produced the following results:

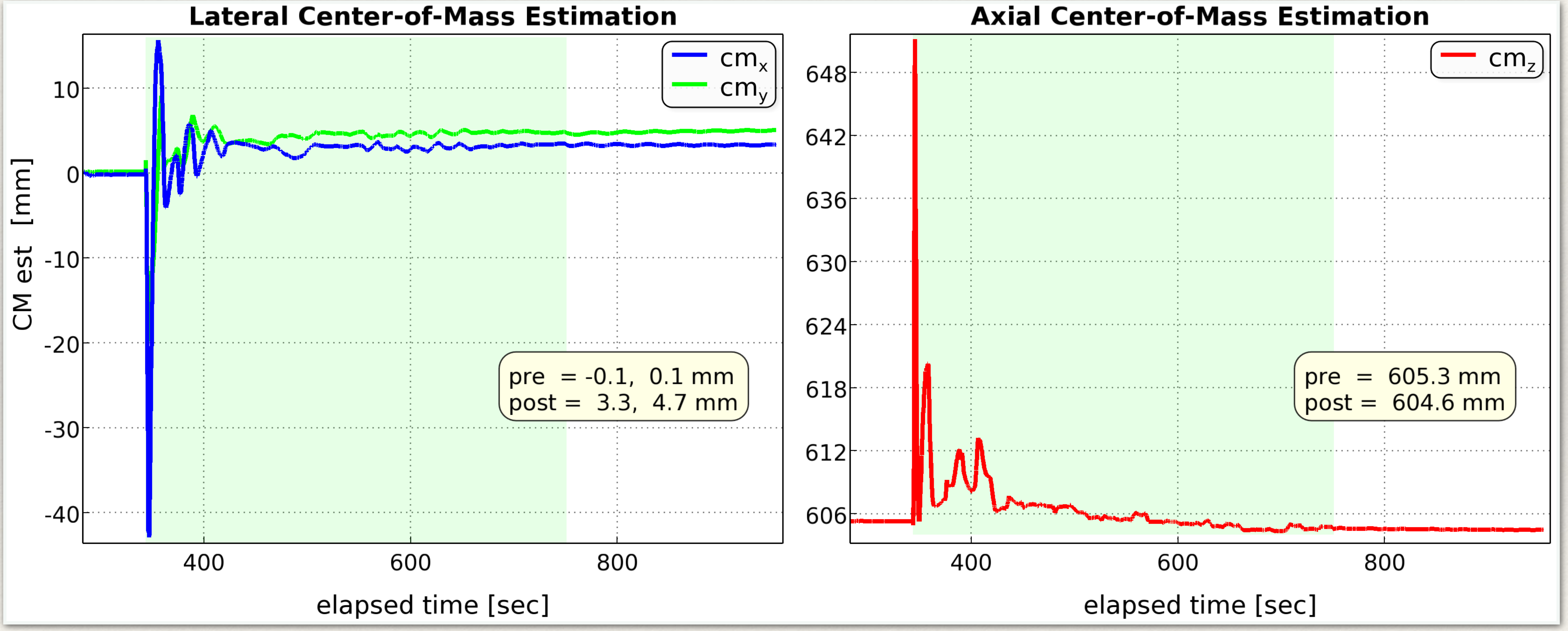

System ID: MMS1 EA019 Flight Results

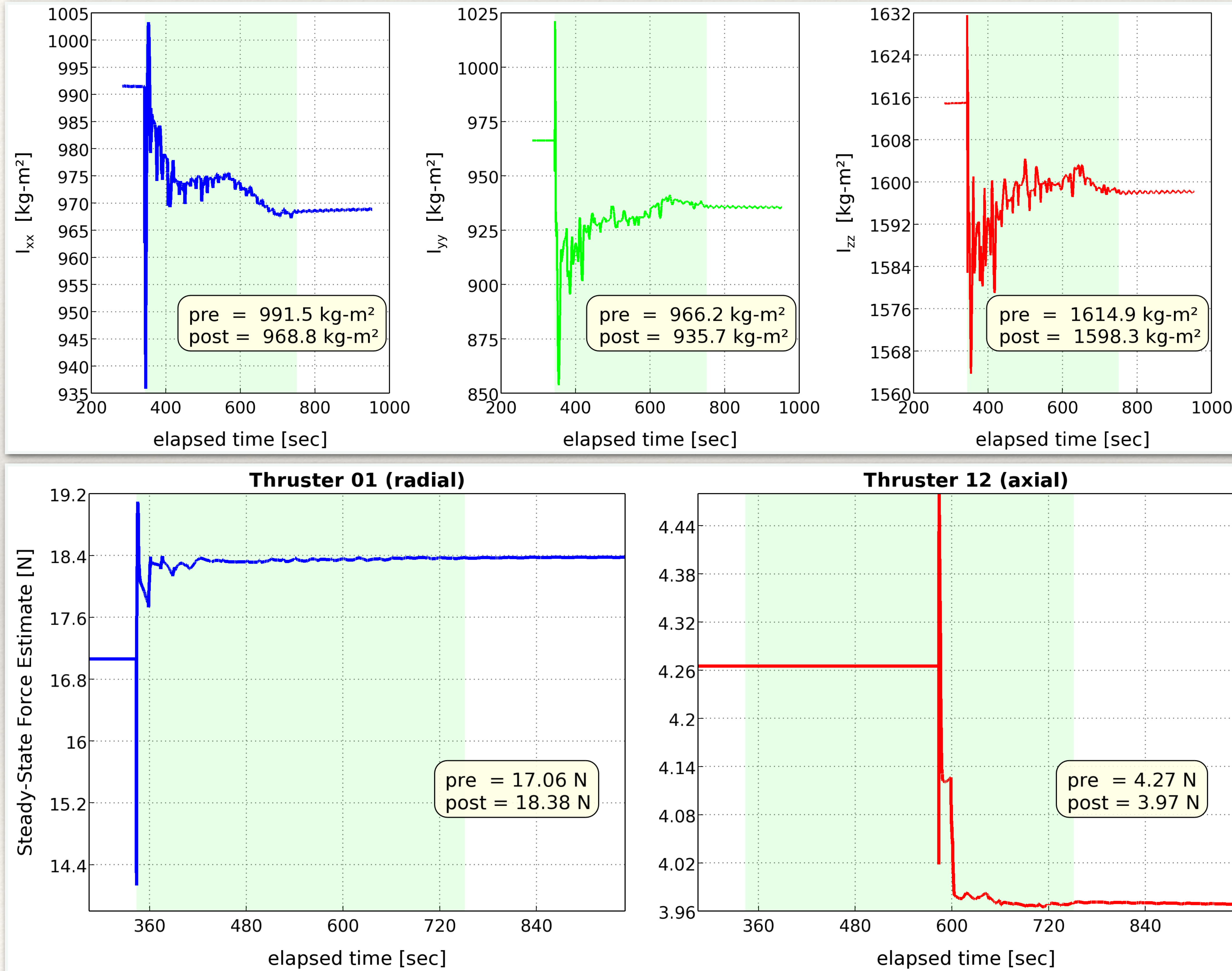

System ID: MMS1 EA019 Flight Results

Comparison of pre-flight and post-calibration system identification for observatory MMS1

State	Units	Pre-Cal	Post-Cal	Difference	
CM-x	mm	-0.14	3.31	3.45	—
CM-y	mm	0.13	4.72	4.59	—
CM-z	mm	605.28	604.56	-0.72	—
Ixx	$kg\text{-}m^2$	991.50	968.10	-23.40	(-2.4%)
Iyy	$kg\text{-}m^2$	996.25	936.54	-59.71	(-6.0%)
Izz	$kg\text{-}m^2$	1614.93	1598.41	-16.52	(-1.0%)
Ixy	$kg\text{-}m^2$	-107.49	-82.88	24.61	(-22.9%)
Ixz	$kg\text{-}m^2$	-0.01	-0.18	-0.17	—
Iyz	$kg\text{-}m^2$	-0.07	-0.30	-0.23	—

Thruster	Units	Pre-Cal	Post-Cal	Difference	
01	N	17.06	18.38	1.32	7.73%
02	N	17.06	18.20	1.14	6.66%
03	N	17.06	18.26	1.20	7.04%
04	N	17.06	18.24	1.18	6.90%
05	N	17.06	18.64	1.58	9.25%
06	N	17.06	18.74	1.68	9.85%
07	N	17.06	18.49	1.43	8.35%
08	N	17.06	18.34	1.28	7.51%
09	N	4.27	3.94	-0.33	-7.67%
10	N	4.27	4.03	-0.23	-5.46%
11	N	4.27	3.82	-0.44	-10.34%
12	N	4.27	3.97	-0.30	-6.94%

Additional Flight Validation

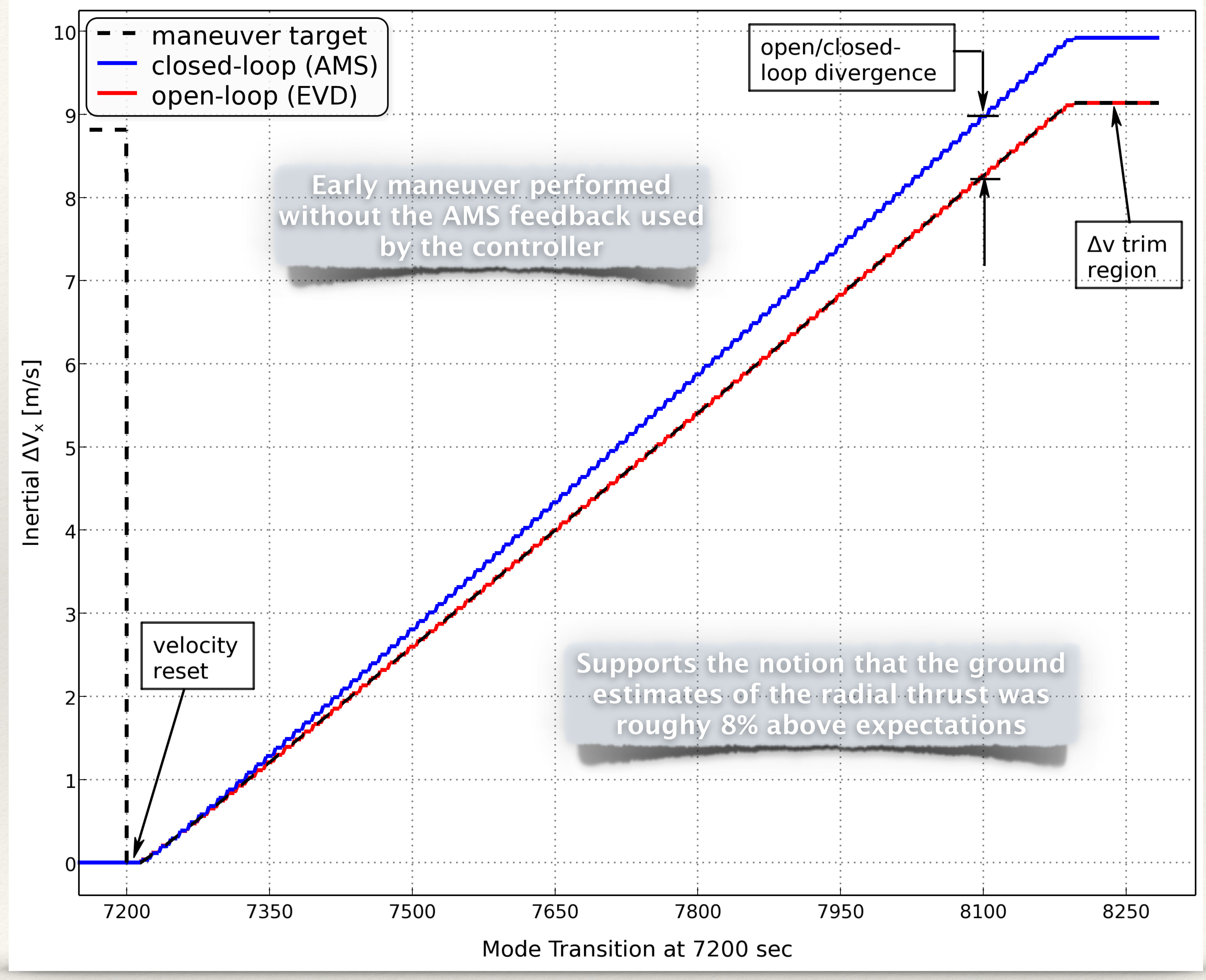

Summary

- **Implementation details with regards to the MEKF formulation were discussed**
- **The MMS on-board attitude and rate estimation MEKF was documented, and flight results presented**
- **An augmented state MEKF for ground-based estimation of thruster output, center-of-mass, moments-of-inertia, and accelerometer biases was developed**
  - a simple two-pulse test-case results were shown
  - Monte Carlo performance statistics were presented for a full calibration of the twelve MMS thrusters
  - Flight system identification results from the MMS EA019 calibration maneuver were shown and compared to pre-flight system knowledge

Thank you for your attention.

Many thanks to our conference organizers for a wonderful event.

Any questions?